AD_____

Award Number: W81XWH-11-2-0163

TITLE: Absorbable Antimicrobial Battlefield Hemostat

PRINCIPAL INVESTIGATOR: Julia Zhao

CONTRACTING ORGANIZATION: University of North Dakota
Grand Forks, ND 58203-9037

REPORT DATE: April 2013

TYPE OF REPORT: Final

PREPARED FOR: U.S. Army Medical Research and Materiel Command
Fort Detrick, Maryland 21702-5012

DISTRIBUTION STATEMENT: Approved for Public Release;
Distribution Unlimited

The views, opinions and/or findings contained in this report are those of the author(s) and should not be construed as an official Department of the Army position, policy or decision unless so designated by other documentation.

The report below provides a complete description of the progress that we have achieved at this point against each of the project objectives.

REPORT DOCUMENTATION PAGE

Form Approved
OMB No. 0704-0188

1. REPORT DATE	2. REPORT TYPE	3. DATES COVERED
April 2013	Final	19 September 2011- 18 March 2013

4. TITLE AND SUBTITLE
Absorbable Antimicrobial Battlefield Hemostat

5a. CONTRACT NUMBER

5b. GRANT NUMBER
W81XWH-11-2-0163

5c. PROGRAM ELEMENT NUMBER

6. AUTHOR(S)
Julia Zhao

email: jzhao@chem.und.edu

5d. PROJECT NUMBER

5e. TASK NUMBER

5f. WORK UNIT NUMBER

7. PERFORMING ORGANIZATION NAME(S) AND ADDRESS(ES)
University of North Dakota
Grand Forks, ND 58203-9037

8. PERFORMING ORGANIZATION REPORT NUMBER

9. SPONSORING / MONITORING AGENCY NAME(S) AND ADDRESS(ES)
U.S. Army Medical Research and Materiel Command
Fort Detrick, Maryland 21702-5012

10. SPONSOR/MONITOR'S ACRONYM(S)

11. SPONSOR/MONITOR'S REPORT NUMBER(S)

12. DISTRIBUTION / AVAILABILITY STATEMENT
Approved for Public Release; Distribution Unlimited

13. SUPPLEMENTARY NOTES

14. ABSTRACT
Uncontrolled bleeding on the battlefield results in a 90% mortality rate within the first hour. Unfortunately, in combat operations, such medical intervention within the golden hour is not always possible, and 50% of battlefield deaths are still due to traumatic hemorrhage. The injury and continued bleeding of the compromised patient needs novel hemostats. A potential solution to this problem is an effective battlefield hemostat that can be resorbed by the body without the requirement for device removal. The object of this proposal is to develop nanomaterial hemostat based on silica nanofibers. Nanosys Inc. and University of North Dakota (UND) have built some platforms to move to the next step by improving the antimicrobial efficacy of the dressing and subsequently, improving its resorptive properties ensuring that this dressing becomes a complete solution for DoD. Our research results suggest that the nanofibers can be resorbed but we would likely need to limit the amount of material left in for effective resorption. The silicon nanofibers did not cause any major irritation, toxicity, and/or inflammatory response, and may represent new formats of hemostat materials that can quickly and effectively stop bleeding at the battlefield.

15. SUBJECT TERMS- none provided

16. SECURITY CLASSIFICATION OF:			17. LIMITATION OF ABSTRACT	18. NUMBER OF PAGES	19a. NAME OF RESPONSIBLE PERSON
a. REPORT	b. ABSTRACT	c. THIS PAGE			USAMRMC
U	U	U	UU	25	19b. TELEPHONE NUMBER *(include area code)*

Table of Contents

Page

INTRODUCTION

Uncontrolled bleeding on the battlefield results in a 90% mortality rate within the first hour, the Golden Hour, a statistic that has remained unchanged since the Civil War. Unfortunately, in combat operations, such medical intervention within the golden hour is not always possible, and 50% of battlefield deaths are still due to traumatic hemorrhage. Thus, the advanced hemostatic products are a critical and invaluable tool that will result in saved lives. However, the major drawback of the current hemostatic products is that the dressing must be completely removed within 24 hours to avoid infection and other significant effects. This removal results in a reopening of the injury and continued bleeding of the compromised patient. A potential solution to this problem is an effective battlefield hemostat that can be left *in situ*, combats infection and can be resorbed by the body without the requirement for device removal and debridement. The object of this proposal is to develop such a hemostat. Nanosys Inc. has previously developed a baseline dressing. With the expertise of the University of North Dakota (UND), this project is now in a position of advancing the baseline to the next step by improving the antimicrobial efficacy of the dressing and subsequently, improving its resorbtive properties ensuring that this dressing becomes a complete solution for DoD. The scope of the work includes five goals. (1) Functionalize nanofibers with antibiotic molecules and demonstrate the antimicrobial activity and retention of the hemostatic efficacy**.** (2) Develop methods of synthesis and demonstrate that nanofibers can be manufactured at >100 g/day. (3) Develop a process for integrating nanofibers into resorbable dressing materials that can produce >200 bandages/day. (4) Determine whether the integrated nanofiber hemostat has any toxic effects to cells or tissues. (5) Demonstrate that antibiotic nanofiber hemostats maintain hemostatic efficacy *in vivo*. *The in vivo* efficacy of the antibiotic nanofiber hemostats will be evaluated using a standard swine liver injury model. Develop appropriate protocols for determining biocompatibility and resorbability of antibiotic nanofiber constructs.

BODY

Y1 Objective 1 Develop a fully resorbable/biocompatible carrier matrix and modify attachment processes appropriately to integrate this matrix with hemostatic nanofibers.
Utilize standard liver biopsy punch model to screen candidate materials and utilize relevant tools to fully characterize the integrated material. Months 1-12

This task was initiated utilizing nanofibers that were grown from Nanosys scaled up nanofiber growth processes described in Objective 4 below. The initial emphasis has been to adapt the roll to roll dip coating process, developed for Nanosys non-resorbable nanofiber hemostat, to be effective for the resorbable constructs. Because of its ready availability they have focused initial efforts on using gelatin sponges as the initial test resorbable scaffold. Initial work was hampered by the fact that commercially available gelatin sponges are somewhat brittle and not amenable to a roller system – however they could be effectively coated using a simple dipping (figure 1). Additionally a thinner version of the gelatin sponge was identified to be more amenable to processing through the dip coating system (figure 2).

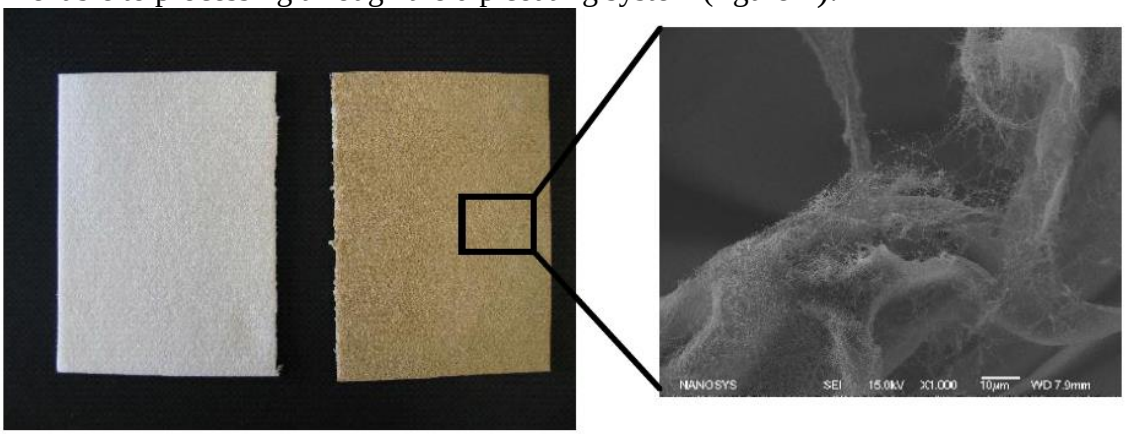

Figure 1: Dip-coated gelatin sponges. The image on the left show uncoated (L) and coated (R) samples of gelatin sponge. The Image on the right is a scanning electron microscope image showing the nanofibers coating on the gelatin sponge at 1000X magnification.

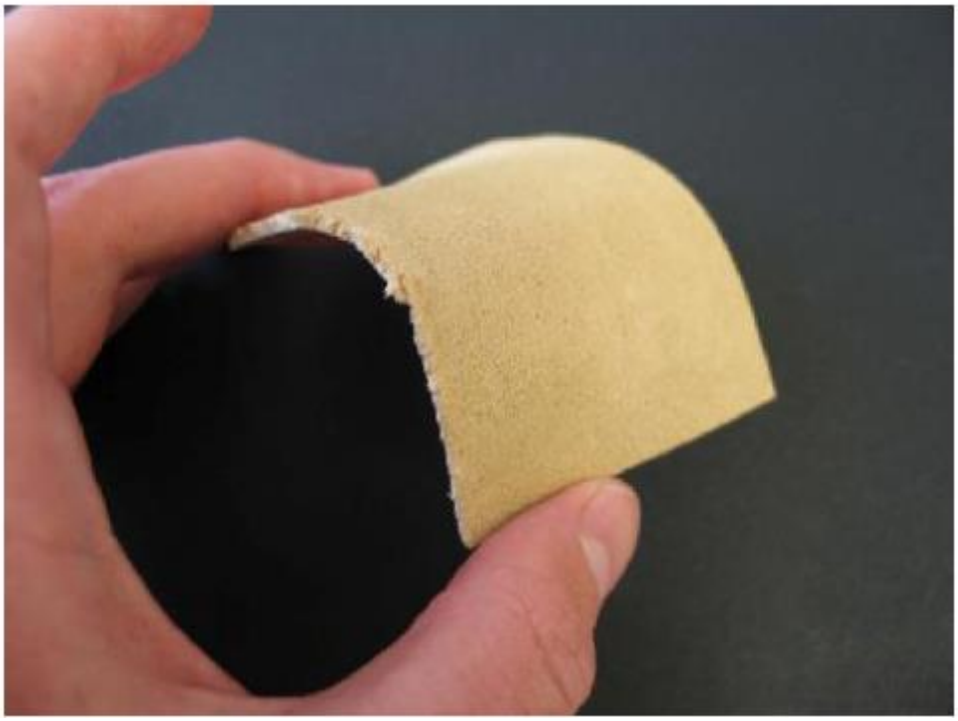

Figure 2: Thinner gelatin sponge that is amenable to roll-roll dip coating process.

In addition to the gelatin sponge, two further resorbable materials were evaluated: a flexible collagen pad and a resorbable carboxymethylcellulose material. Both of these materials were easy to coat and had excellent handling properties. Figure 3 below shows images of all three materials in coated and uncoated form. In order to insure that different material scaffolds are coated at the same nanofibers density, we have adopted the following qualification procedure:

1. The scaffold materials is first cut to a 10cm x 10cm pad and weighed. The pad is then completely immersed in the solvent used for coating the dressing – reagent alcohol. After immersion, the dressing is removed and the excess solvent allowed to drain for 10 seconds. The dressing is then weighed a second time and this allows calculation of the volume of solvent absorbed by the dressing.
2. For coating our initial materials, we have selected a nanofiber coating density of 0.5mg nanofibers per square centimeter of dressing. This is based upon prior work carried out using our product (ATD **no defined**) that determined that the hemostatic efficacy plateaued at approximately this density of nanofibers.
3. Therefore if a dressing material absorbed 10ml of solvent in step 1 this would mean that this dressing material has a solvent absorption capacity of 100 microliters per square centimeter. Therefore, to load the dressing at a nanofiber density of 0.5mg per square cm, the nanofiber concentration in the solution should be 0.5mg per 100 microliters (or 5mg/ml) in the solvent.

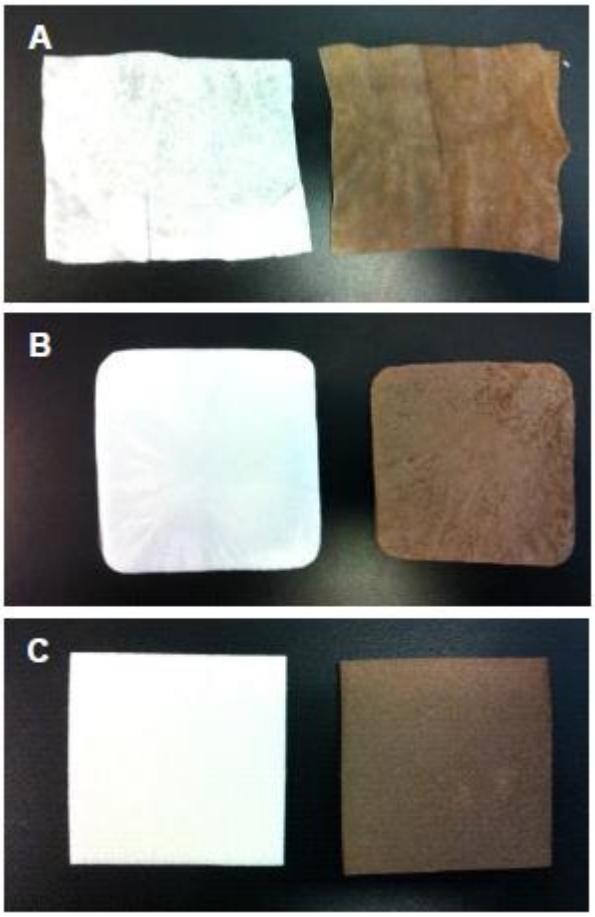

Figure 3: Images of the three materials coated using the dip coating process we have developed. In each case the images show uncoated material (left) and coated material (right). A: This is a carboxymethylcellulose dressing that the manufacturer claims is soluble – we will investigate this claim. B: Collagen pad. Note the change in size of the pad post processing. This indicates some change to the material caused by our coating

process. C: Gelatin sponge. This thin (2mm) gelatin sponge material coats well and material appearance and handling is unaffected by the coating process.

The approach described here for coating the scaffolds with nanofibers was essentially the basis of the scaled up approach described in section 4 below.

***Subtask 1b Evaluate selected constructs* in vivo.**

In order to evaluate the hemostatic efficacy we tested these three substrates in our standard swine injury model. A biopsy punch was employed to create 5 mm diameter, 8 mm depth wounds on the exposed liver of swine. The material to be evaluated was then placed over the injury area and lightly held in place. Every thirty seconds the light pressure is removed and the injury is monitored to see if blood continues to seep through or around the applied dressing swab. Excess blood flowing through or around the device was collected with gauze pads. The time at which no further bleeding can be seen through or around the dressing swab was determined as the time to hemostasis (TTH).

Previous work has shown that in the absence of a hemostatic agent in the dressing material bleeding continues for >300 seconds. Effective hemostasis is nominally set as a device that results in an average time to hemostasis of <150secs.

Figure 4 below shows the data collected from at least 10 separate wounds evaluated for each material. As a positive control we used the Advanced Trauma Dressing (silicon nanofibers incorporated into a carboxymethylcellulose dressing that has been shown as an effective hemostat in this model). As can be seen from the data all of the new nanofiber coated dressings were effective hemostatic dressings. The gelatin sponge was particularly effective with an average time to hemostasis for the 10 injuries of <70secs. This excellent performance likely reflects the benefit of having the hemostatic nanofibers in an absorbent sponge-like dressing that has a good capacity to absorb much of the initial bleed and initiate coagulation before the dressing is dislodged. The collagen nanofiber pad is less absorbent and thus, when the bleeding was heavier, had a tendency to dislodge and prevent effective adhesion of the applied device to the injured organ.

As a result of the data collected here the gelatin sponge appears to be the promising material. Not only is the dressing an effective hemostat but also a well established surgical dressing material with a well understood biocompatibility and dissolution profile. We recommend that this combination of silicon nanofibers and gelatin sponge scaffold is the construct most appropriate for continued development and assessment in more clinically relevant models. This dressing was used as the test article in the sections below where evaluation of the biocompatibility and dissolution of implanted material was evaluated.

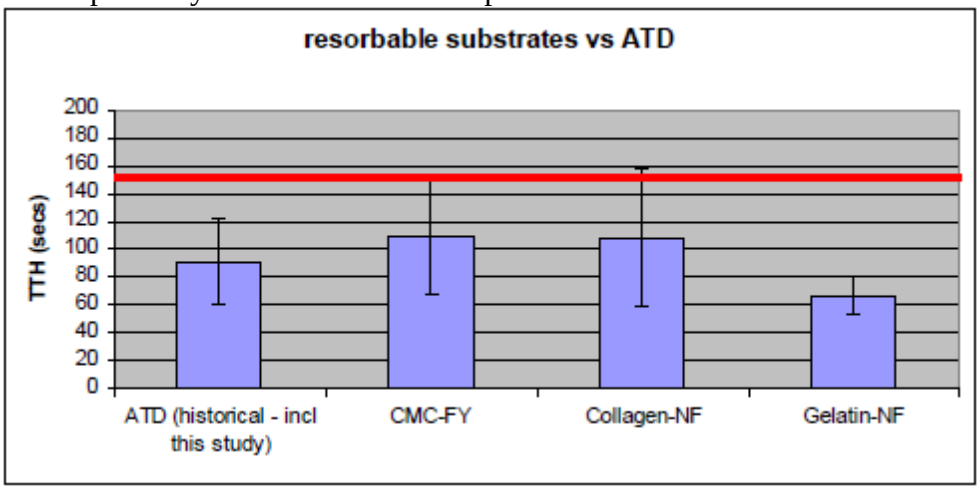

Figure 4: This graph shows the average time to hemostasis for nanofibers coated CMC constructs in our standard swine injury model. Each bar represents the mean +/- SD of the time to hemostasis for 10 independent injuries. As the data shows the average time to hemostasis for both constructs is well below the cut-off criteria of 150 secs (red line), indicating that the nanofibers produced from the scaled up processes are hemostatically effective.

Y1 Objective 2 Empirically demonstrate resorption of the nanofiber dressing in situ and evaluate material safety. Determine if the integrated nanofiber hemostat has any toxic effects to cells or tissues using cell based and small animal models. Months 6-12

This objective was broken down into three sections. Firstly we evaluated the intrinsic capability of the silicon nanofibers to dissolve. Secondly we have initiated a study to demonstrate that the gelatin sponge/nanofiber dressing construct will be well tolerated and dissolved when implanted. Finally we have evaluated whether the silicon nanofibers or the nanofiber/dressing construct have any toxic effects.

In order to demonstrate that the silicon nanofibers have an intrinsic capability of dissolving over time in a physiologically relevant solute, we carried out the following experiment:

Silicon nanofibers immobilized on silicon wafers were immersed in a saline solution and stored at 37^{o}C to mimic physiological conditions. The saline solution was replaced every week and the surface of the wafer was examined at weekly intervals to determine the dissolution rate of the nanofibers.

As figure 5 shows the SEM images of the nanofibers after 4 and 8 weeks indicate that there is clear dissolution of the nanofibers compared to the control sample. This dissolution over time is further confirmed after 12 weeks when the wafers were removed from solution and examined visibly. As figure 6 shows the nanofibers had completely disappeared after 12 weeks in saline solution.

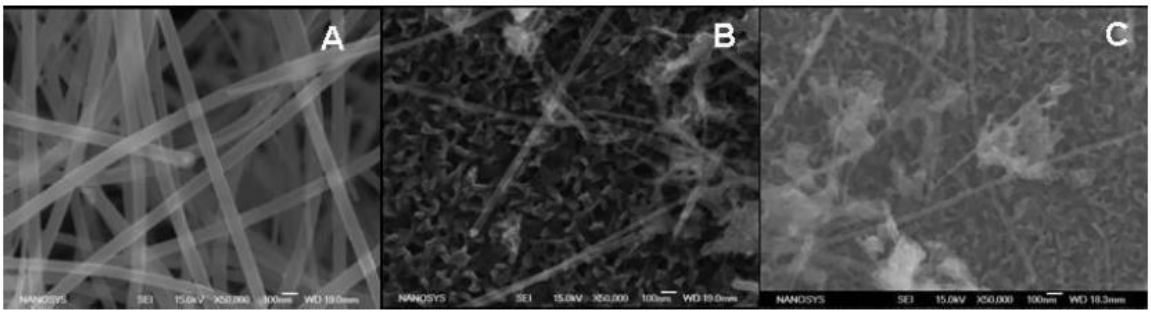

Figure 5. SEM images of nanofibers immobilized on a wafer surface. Panel A shows the nanofibers prior to exposure to saline solution. Panel B shows a selected region of the wafer after 4 weeks in solution and panel C a different region after 8 weeks in solution. Clear dissolution of the fibers can be seen and notice that in general nanofibers that remain after 8 weeks in saline are thinner and have a rougher surface than those exposed for 4 weeks, indicating the loss (dissolution) of the coated material.

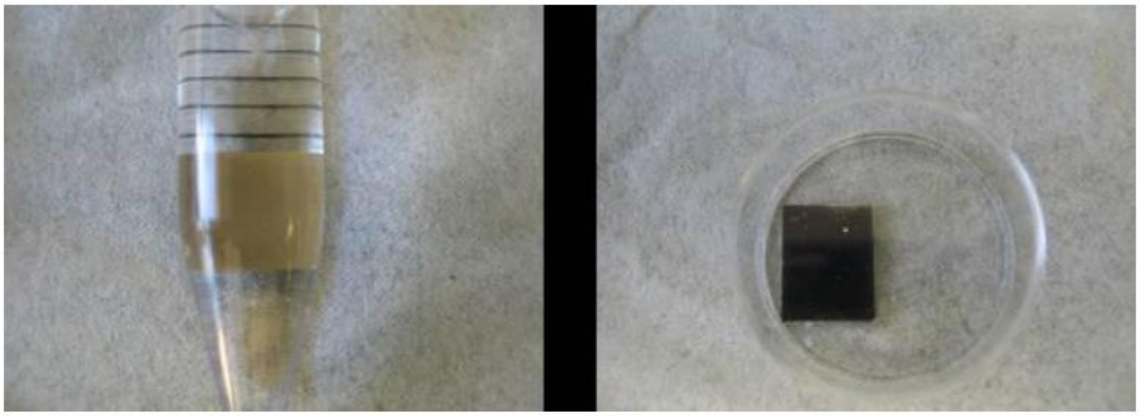

Figure 6. The image on the left shows the silicon fibers immobilized on the wafer substrate 1 day after being placed at 37° C. After 12 weeks the wafer was removed and photographed again – as the image on the right shows the tan-colored nanofibers are no longer present on the surface of the wafer.

This experiment demonstrates that the nanofibers can dissolve over time. However, actual implantation into an animal is needed to determine whether this dissolution could be increased or decreased when it occurs *in situ*. Generally for most implanted materials to be considered non-permanent it is desirable if the resorption were to occur within 4-6 weeks**.** Therefore we set out to design an appropriate study to evaluate this.

Although we can see that the nanofibers will dissolve over time in an *in vitro* system, where the fluids are replenished, and there is plenty of solute, it is unknown if the material will also dissolve or be resorbed in a defined implantation site.Therefore we selected a rabbit subcutaneous implantation model to determine whether the nanofibers and the gelatin carrier would dissolve. In designing this study we determined that actual amount of resorption might be difficult to quantify. In order to mitigate this problem, we have set up a study outlined in detail below.

Study 1 – Histological determination of remaining implanted material

For this study we selected 3 sizes of implant ranging from 0.5" diameter to 0.125" diameter. For each size the implanted material will consist of a gelatin sponge coated with nanofibers and an uncoated gelatin sponge control. The study will be carried out by the independent accredited laboratory service company NAMSA located in Northwood, OH. Nine rabbits (3 rabbits for each of the three time points 2, 4 and 8 weeks) will be implanted at 12 sites each (2 of each size test article will be implanted = 2 x (3 different sizes of coated + 3 different sizes of uncoated =12 sites per animal). The experiments will be terminated at 2, 4 or 8 weeks and the animals euthanized at 2 weeks will also have a time zero implant placed at this time to act as a baseline control for comparing resorption. The implant sites will be excised and paraffin embedded and stained with H&E. The sections will then be evaluated microscopically for evidence of resorption. This study is currently ongoing and we will prepare an addendum to this report to fully describe the results of this study.

In year 2 quarter 1 and 2 (or representing our interim final report as we have requested no-cost extension to October to fully accomplish our proposed specific objectives), we have obtained valuable data of resorption which were produced from the independent accredited laboratory service company NAMSA located in Northwood, OH as a contract. The data were encouraging as gelatin-coated NF hemostats have been all or almost all resorbed in the tissue of rabbits (3 per group), while the resorption rate of larger hemostat is lower than that of the smaller hemostat or uncoated controls. However, resorption of coated hemostats with a smaller diameter (0.8 cm) was almost comparable to the control without coating. The overall tendency indicates that absorption/resorption is size dependent. These novel findings will help design new approaches to screening hemostats or other in vivo nanomaterials for biomedical applications.

In Q3, we demonstrated that gentamicin functionalized nanofibers were still hemostatic. We continued to evaluate nanofibers functionalized with antimicrobial moeties for their hemostatic activity in this quarter. The Wu lab in UND investigated the mechanism that is associated with cellular responses in the alveolar epithelial cells after treated with modified nanofibers. We detected the toxic effects of gelatin coated-nanofibers on the living cells. The bandage induced-apoptosis was estimated by vybrant assay (Figure 7), and the bandage induced DNA damage was determined by comet assay (Figure 7). The results indicated that apoptosis and DNA damage in MLE-12 cells were induced by bandage coated with silicon nanofibers for 24 hours. We measured the DNA repair proteins response to gelatin coated nanofibers (Figure 8), which showed particular responses by XPB, OGG1, CSB and PUMA but not by APE1 and XPC. These results suggest that specific DNA repair pathways (base excision DNA repair and nuclear excision repair) are involved in nanofiber treatment with *in*

vitro cell culture. In addition, slightly increased PARP1 cleavage was observed, indicating a potential role of the DNA repair protein in repairing oxidative DNA damage by exposing nanofibers.

We found that although the nanofibers induced some toxicity, it is generally moderate without induction of significant cell death. We actually found that nanofibers induced less autophagy (a conserved homeostasis self-eating process to preserve the vital cells during starvation) in MLE-12 cells compared to the controls (Figure 9). These observations suggest that gelatin coated-nanofibers may be relatively safe when applied in biomedical fields, such as nanofiber hemostats.

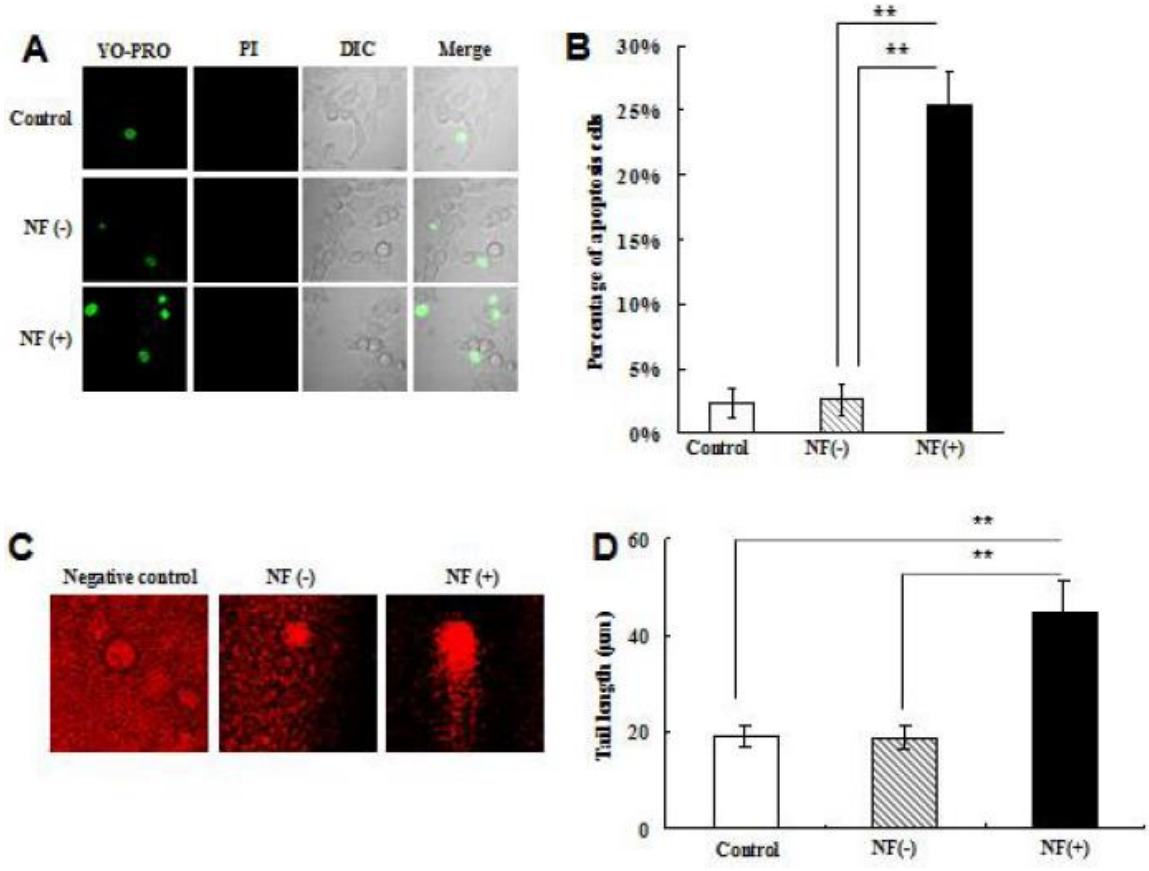

Figure 7. Vybrant assay and Comet assay of the toxic effects of gelatin coated with nanofibers on the cells. (A) Nanofiber-induced apoptosis in MLE-12 cells after 24 h of incubation with the gelatin coated-nanoparticles using the Vybrant apoptosis assay. (B) The data were derived from confocal fluorescence microscopy and the percentage of each type (apoptotic and necrotic) of cells was calculated against the total counts (at least 100 cells were counted in each sample). The data showed here are only apoptotic cells. The data are presented with means±SD. (c) Representative fluorescence image of comet assay of the mice MLE-12 cells following 24 h of incubation with medium (negative control), gelatin coated without (NF (-)) or with silicon nanofibers (NF (+)). (d) Column graph showing the average tail lengths after being incubated with medium (negative control), gelatin coated without (NF (-)) or with silicon nanofibers (NF (+)) for 24 h. Data are shown with means ± SD. All of the data are representative of three experiments.

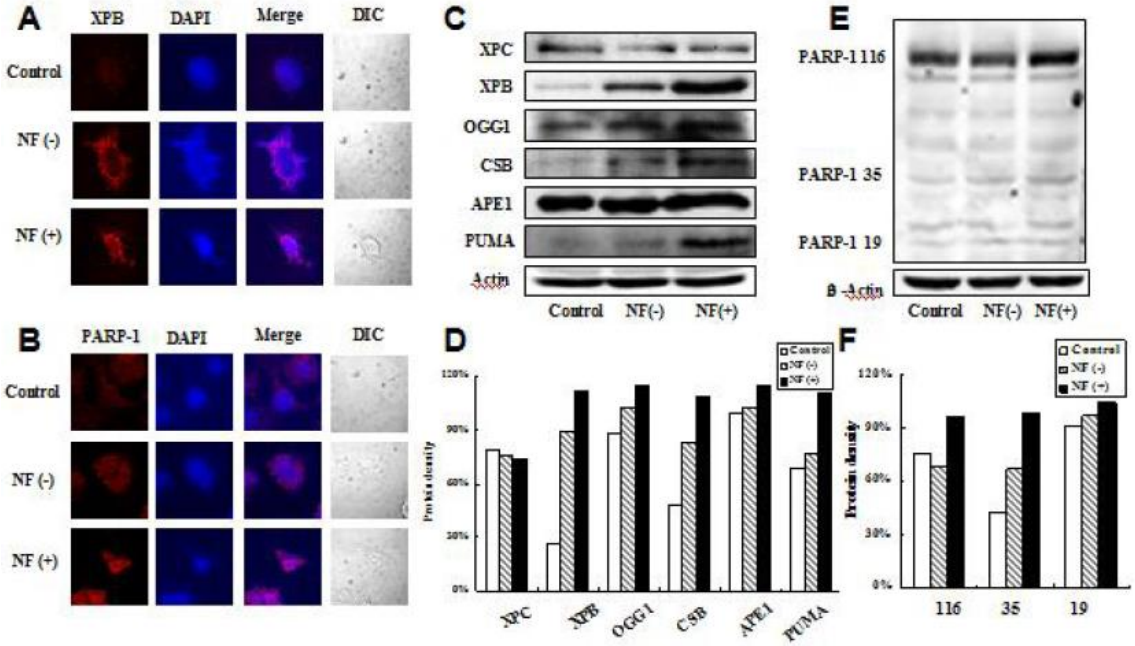

Figure 8. Analysis of the nanofibers' effects on the DNA repair enzyme and signaling proteins. (A, B) Confocal image of nanofiber-induced increase of XPB and PARP-1 in MLE-12 cells after 24 h of incubation with nanofibers (NF-) and gelatin coated nanofibers (NF+). Negative control: PBS only. (C, D) Western blot of various DNA repair and DNA daamge response proteins (XPB, OGG1, PUMA) in response to nanofiber treatment. (E, F): PARP-1 cleavage gel imaging and densitometry quantification.

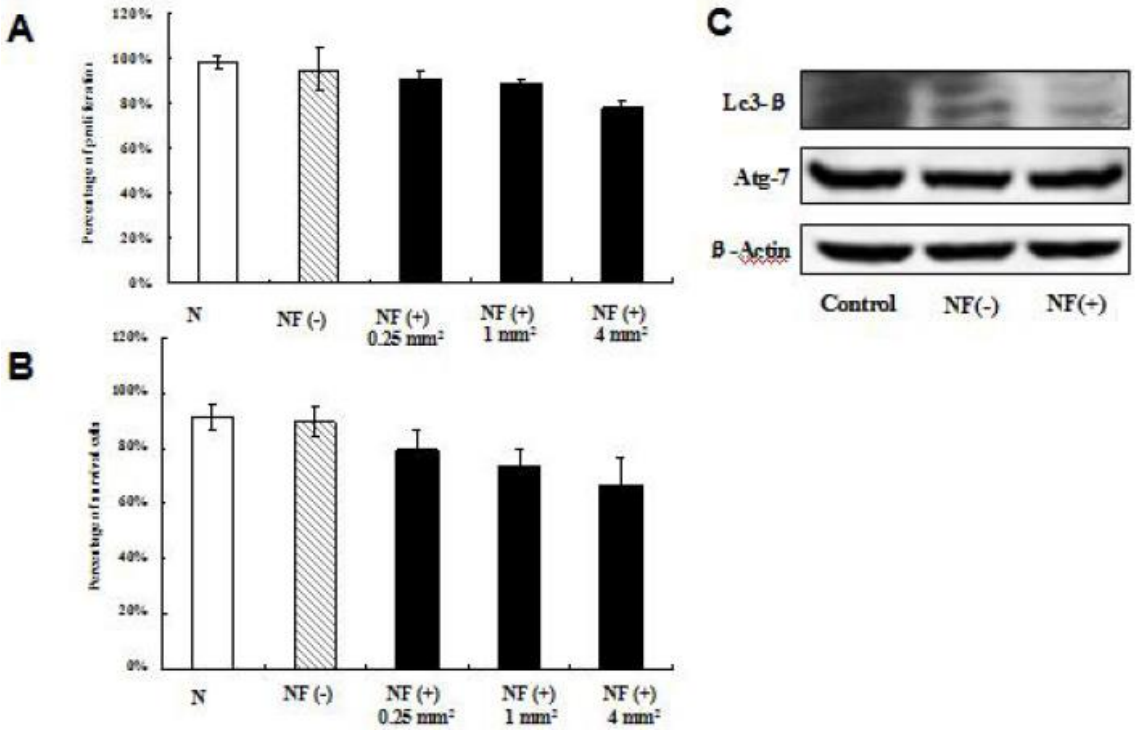

Figure 9. Cytotoxic effects of the nanoparticles. (A) Cytotoxicity on MLE-12 cells after 24 h of incubation with the gelatin coated-nanofibers using the MTT assay. The percentage of surviving cells was inversely related to the increased sizes of nanofibers. (B) Cytotoxicity on MLE-12 cells after 24 h of incubation with the gelatin coatednanofibers using Trypan Blue exclusion assay. The Trypan Blue exclusion assay directly determines the cell death. (C) Autophgy of MLE-12 cells induced by gelatin coated nanofibers.

Y1 Objective 3 Develop and further evaluate various surface functionalization strategies that can primarily improve the hemostatic efficacy of the nanofibers and secondarily allow additional functionality to be attached to the nanofibers (e.g. antimicrobial functionality). Empirically demonstrate the improved hemostatic efficacy and functionality Months 0-9

This task was initiated in Zhao's lab at the UND using silicon nanofibers from Nanosys. Different groups have been added to the surface of silicon nanofibers (SiNFs) by the following procedure:

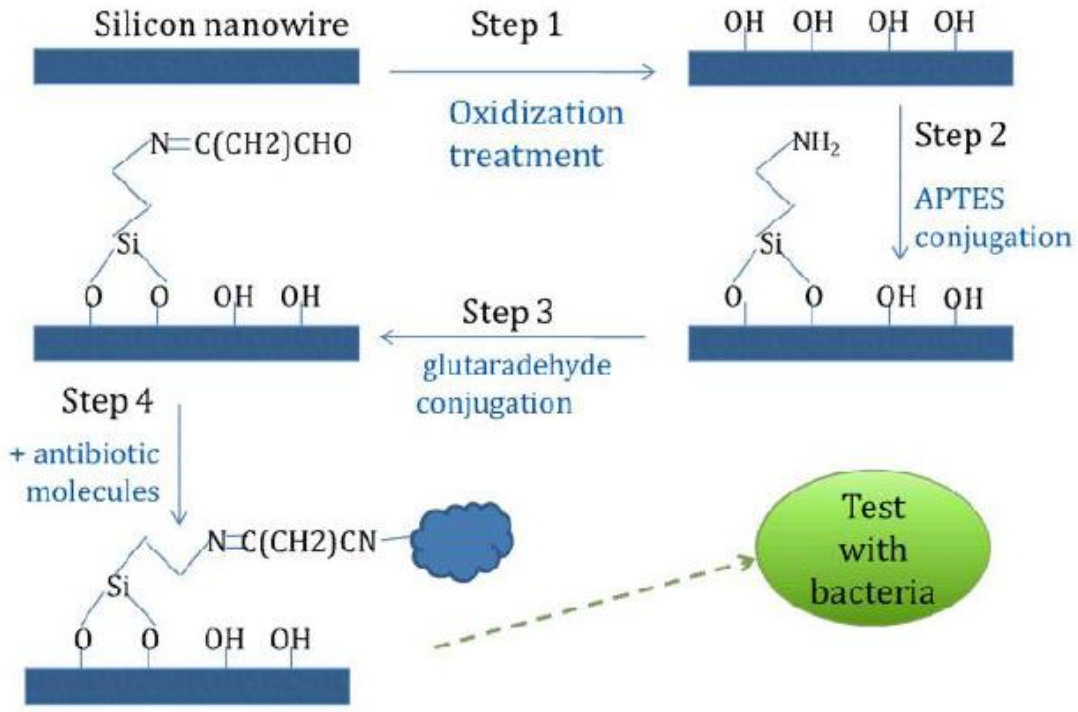

Figure 10, Schematic diagram of SiNWs modification

SiNFs were heated at 500 degree to remove surface oxide layer and organic remains, and then dipped into 1% $NH_3.H_2O$ aqua solution for generation of active OH group on the surface. SEM (Scanning Electron Microscope) image of SiNFs showed that nanofibers have a uniform diameter of about 50 nm and length over 2 μm. After reaction, the new peak at 3500nm^{-1} in FT-IR (Fourier transform infrared spectroscopy) represents O-H group on the surface, which was also confirmed by EDS (Energy-dispersive X-ray spectroscopy) in figure 12. Percentage of oxygen greatly increased from 8.39% to 25.32%.

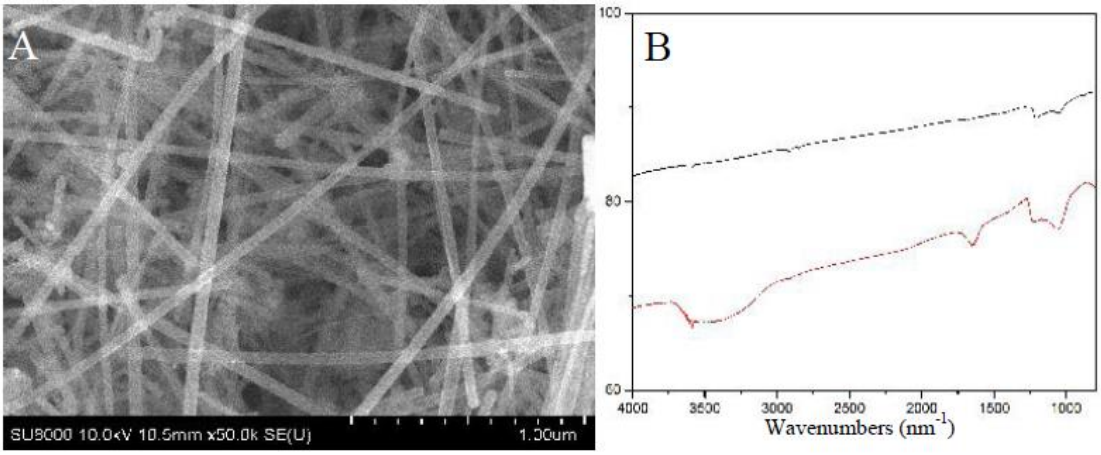

Figure 11, A, SEM image of SiNFs; B, FT-IR of SiNFs (black) and OH_SiNFs (red)

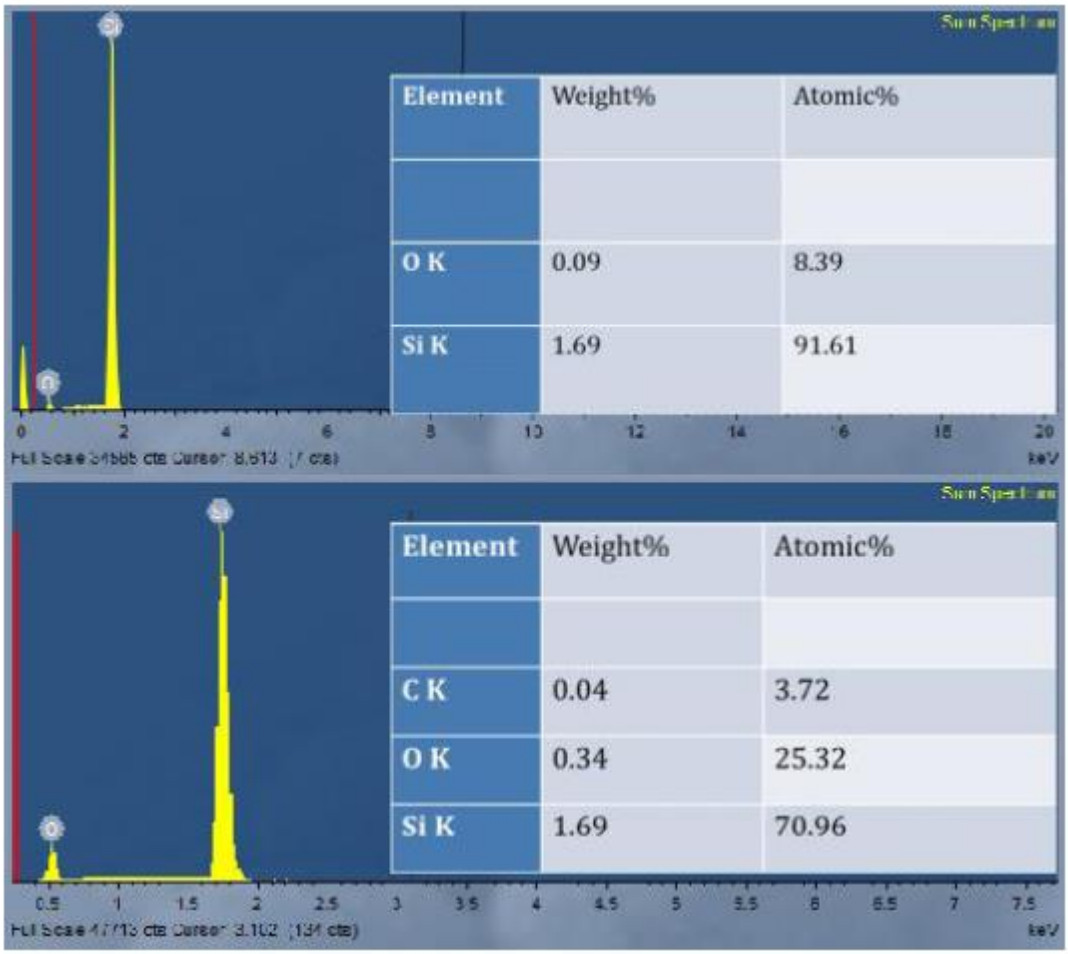

Figure 12, EDS of original SiNFs (up) and OH_SiNFs (bottom).

Then OH_SiNFs were put in 2% APTES ((3-aminopropyl) triethoxysilane)/Acetone solution for 30mins and then washed with acetone thoroughly. In this step APTES would react with -OH group of SiNFs to make a layer of SiO_2 and left amino group on the surface. FT-IR in figure 13 showed several new peaks which indicate the N-H ($3300nm^{-1}$) and C-H ($2950nm^{-1}$) groups. And carbon and nitrogen elements from APTES could be also confirmed by EDS. The efficiency of amino-SiNFs was optimized by changing parameters such as concentration, solvent, temperature and so on.

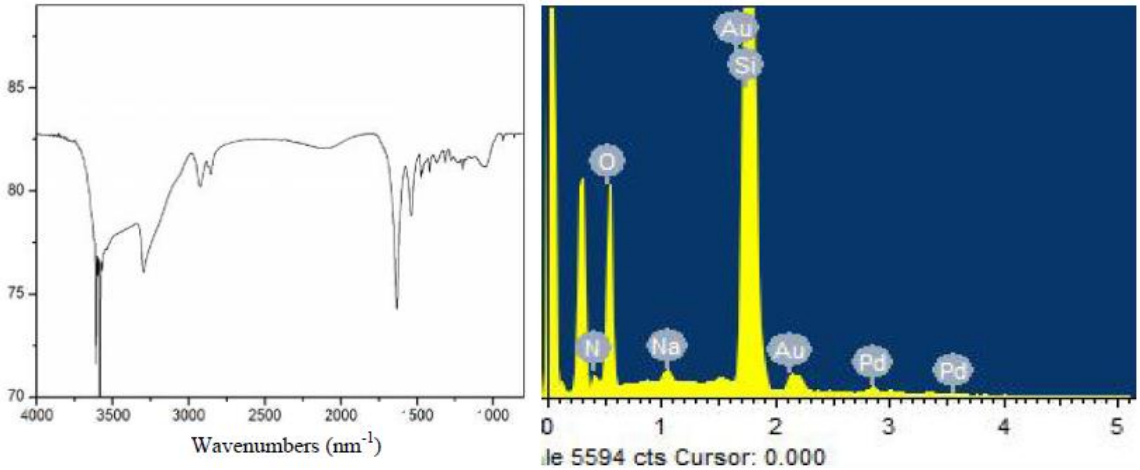

Figure 13, FT-IR (left) and EDS (right) of amino_SiNFs

In order to further modification of antimicrobial group, glutaraldehyde (GA) was chosen to introduce CHO group on the surface of nanofibers. The amino_SiNFs were put in 2.5% GA/H_2O solution for 3 hours with stirring, then washed with distilled water. FT-IR in figure 14 showed one new peak at about 1720 nm^{-1} standing for C=O bond, which meant CHO groups exist on the nanofibers after reaction. Also from the SEM image, the morphology of SiNFs slightly changed compared with figure 11A.

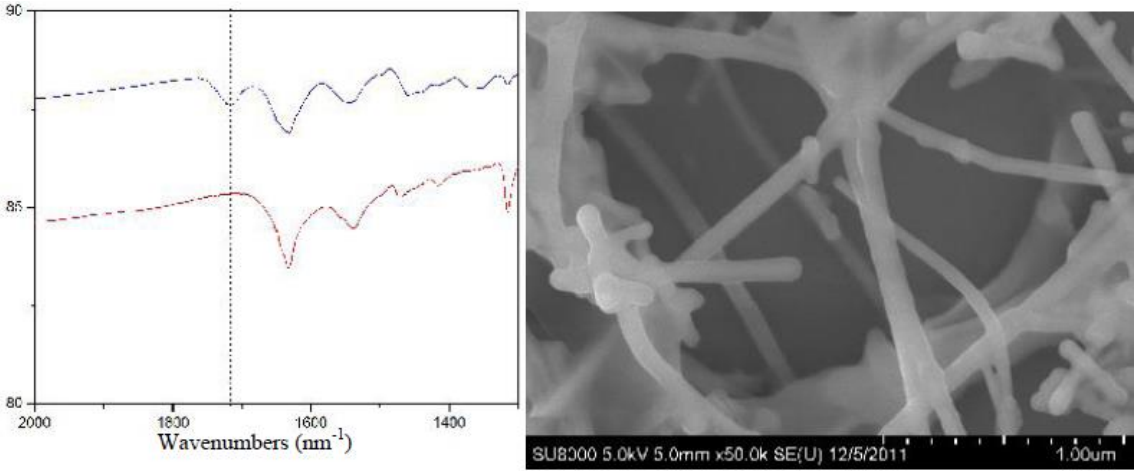

Figure 14, FTIR and SEM image of SiNFs after reaction with GA

The SiNFs were sonicated for 5mins to achieve homogenous dispersion in water, and then mixed with gentamicin aqua solution (10mg/ml) for 2 hours with stirring. After reaction, we test the anti-bacterial property of SiNFs under Dr. Wu’s direction. The detail is followed: first, the original *Pseudomonas aeruginosa* (Pa) bacteria were diluted to 1/1000000, then mixed with gentamicin, unmodified SiNFs, modified SiNFs at the ratio of 15:1. Then the mixed solutions were spread on the LB dish and placed in bacteriological incubator for 9 hours.

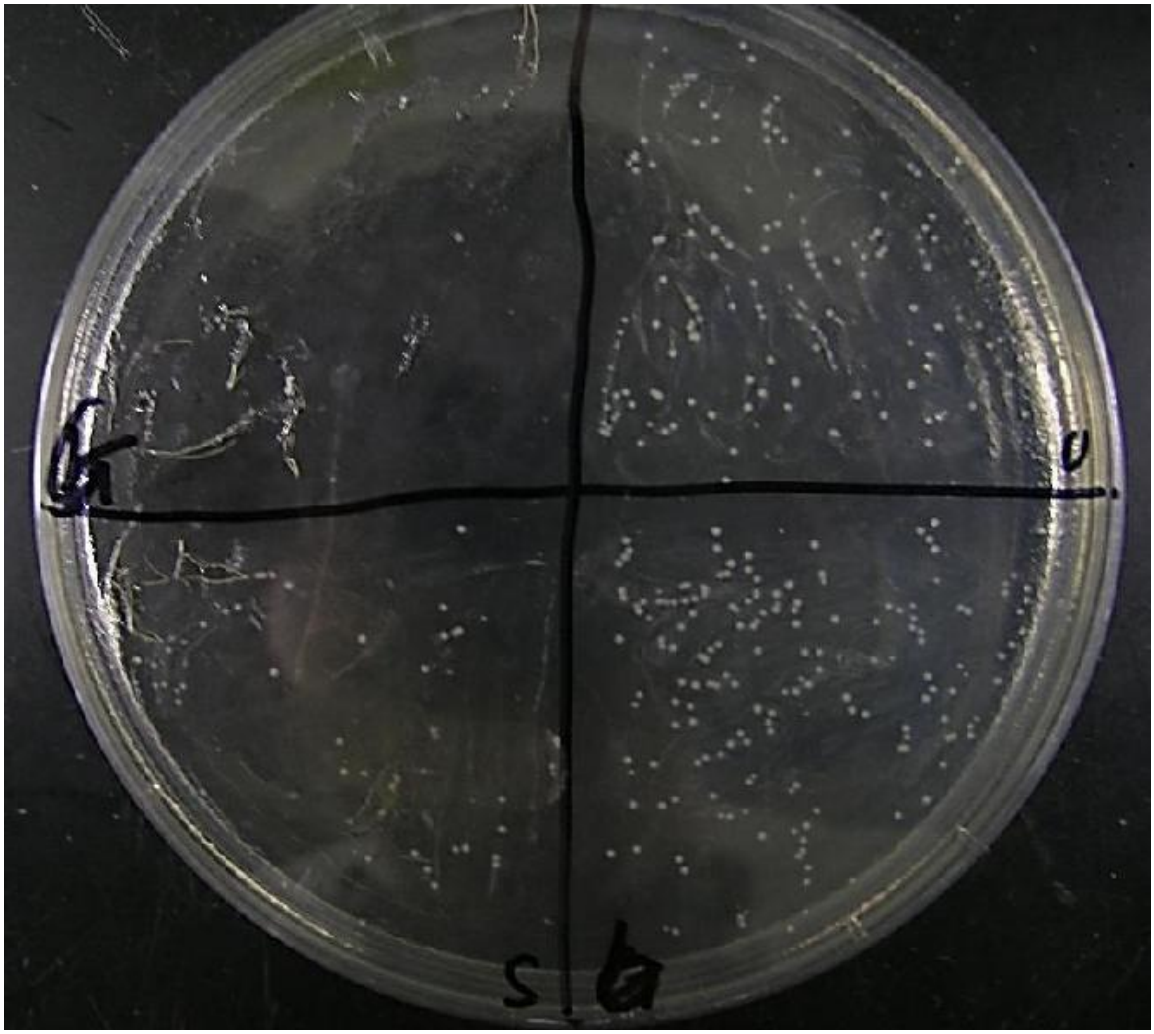

Figure 15, the Pa grownth on PL film with different materials, (G) is gentamicin, (o) is unmodified SiNFs, (s) is modified SiNFs, (b) is blank.

Figure 15 showed bacteria growth in different area on LB dish. The white dots were colonies on the dish. For the gentamicin, we could not find any colonies in up-right area which showed gentamicin have great antibacterial effect. It is clearly that the growth of Pa in the up-right area (unmodified SiNFs) and down-right area (Blank) is almost the same; it means the unmodified SiNFs have no antibacterial property. At the meanwhile the quantity of colonies in down-left area (modified SiNFs) significantly decreased compared to unmodified SiNFs. Therefore, it confirmed that the gentamicin was successfully grafted on the surface of silicon nanofibers and the bactericidal activity retained. Simultaneously by counting quantities of colonies under different gentamicin concentrations (figure 16), we calculated the weight ratio of gentamicin and nanofibers is about 2-4:10.

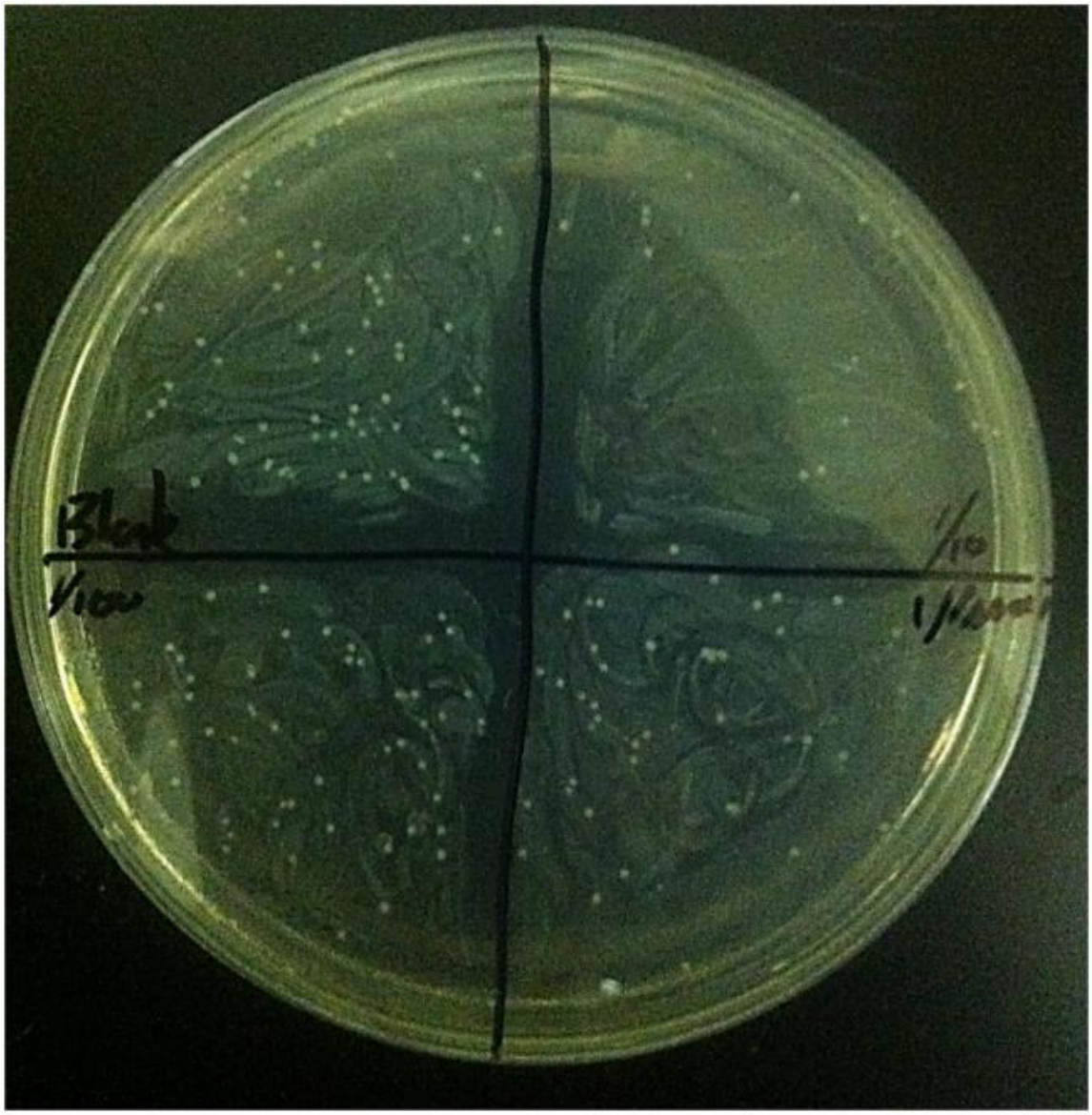

Figure 16, PA growth on LB film with different concentrations of Gentamicin.

Hemostatic efficacy of modified nanofibers.

One important question to address is whether the functionalization of the nanofibers surface affects the ability of that surface to initiate coagulation. In order to evaluate this we tested the ability of nanofibers to activate coagulation of whole pigs blood. The method used was to add 2.5ml of pigs blood to 10mgs of either unmodified nanofibers or nanofibers functionalized with gentamicin (as described above) and measure the rate of coagulation using an ACT analyzer. This system measures the change in mechanical deflection of a marker in a test tube to determine the rate of clot formation.

Using this method we measured each type of material 3 times and the results are shown in Figure 17. As the data shows, using this concentration of nanofibers in whole blood we were unable to detect a difference in coagulation rate using unmodified or gentamicin functionalized nanofibers. Both were effective activators of coagulation (typical activated clotting times of whole pigs blood using a kaolin clay activator are approximately 90 seconds, in the absence of activator the blood will remain unclotted for over 300 seconds). Thus the functionalization of nanofibers by antibiotic coating has not altered the clotting potential, suggesting a promising way to develop antimicrobial hemostat materials for battlefield applications. **Despite the progress,**

we are attempting to reproduce these data in the last few months. Hopefully we will be able to obtain improved data soon.

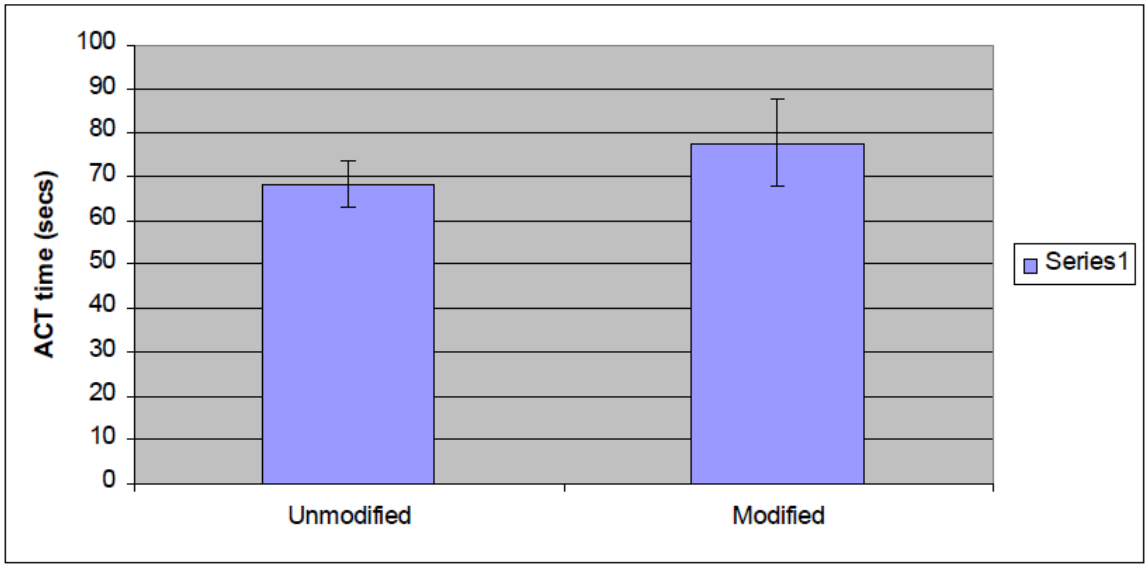

Figure 17 The bars show the average activated clotting time (in seconds) for pigs blood either activated by unmodified nanofibers (left) or gentamicin functionalized nanofibers (right). As the data shows both materials activate the clotting of blood within 80 seconds and although the average time for unmodified nanofibers is slightly faster this is not statistically significant.

Y1 Objective 4 Demonstrate that nanofibers can be manufactured at >100 g/day and demonstrate a process for integrating nanofibers into resorbable dressing materials that can produce >200 bandages/day. The particle substrate based approach will be used to increase the yield of nanofibers produced using standard fixed bed reactors. Existing methods for coating materials with nanofibers will be adapted to a roll-to-roll coating method that will allow continuous coating of the dressing materials Months 0-6

A: Scaling up nanofiber production

The standard method used at Nanosys for producing silicon nanofibers was to deposit gold colloid on a flat substrate such as a silicon wafer or glass plate to produce highly crystalline nanofibers in a high temperature CVD (chemical vapor deposition) reactor. However this approach can only yield a few mg's of nanofibers per substrate leading to a limitation of scale. Therefore a major task for this project was to improve the scale of nanofiber production by several orders of magnitude in a cost effective manner.

Initially we leveraged off a planar substrate approach but used a thin stainless steel foil as the substrate for the gold colloid deposition. The foil was then coiled into a spiral, providing a significant surface area for gold deposition and nanofiber growth (see figure 18). Nanosys' largest CVD reactors have a tube diameter of 8" and this allows for ~6 sq. meters of foil to be coiled and placed in the chamber. After nanofiber growth the coiled foil is removed and the nanofibers harvested by sonication into alcohol. The alcohol containing the fibers can then be passed through a 0.45micron filter and the fibers remain on the filter as a flat cake that can then be used as needed. Typical yields for this method are 0.15g nanofibers per sq m foil. This allows approximately 1 g to be produced per 8" furnace run and about 4 runs can be performed in a single shift. We produced multiple nanofiber cakes using this approach and delivered the first samples to UND for initial studies as well as initial samples for developing the matrix coating described above under objective 1.

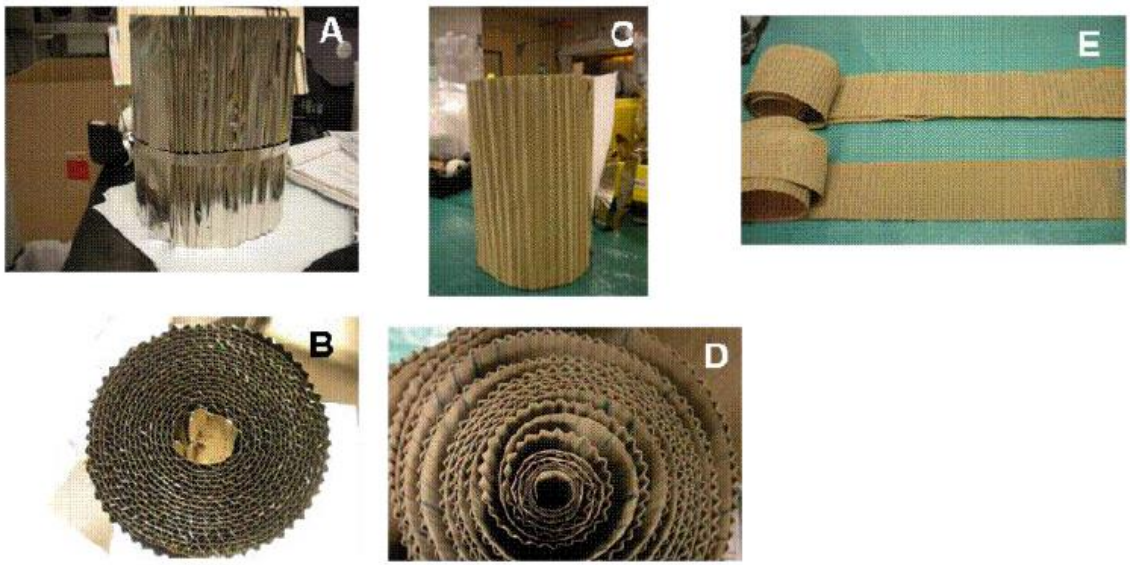

Figure 18: Nanofiber growth on foil substrate. A: side view of stainless steel foil before fiber growth, ready to insert into the tube furnace. B: top down view of foil before growth process. C: side view of the foil substrate post-wire growth, D: top down view of foil substrate post-growth, E: two foils partially unrolled showing the nanofibers growth (brown coloration) along the whole foil.

However this method was still limited in terms of required yield. If we assume each bandage will contain at least 0.1g of nanofibers then we need a process that will allow us to mass produce thousands of bandages per day. This necessitates a process that can yield 100's of grams of nanofibers per day. One approach to achieving this is to dramatically increase the surface area of growth substrate by reducing that substrate in to small particulates. We had previously developed methods for other projects whereby nanofibers can be grown directly on graphite particles yielding up to 100g's of nanofibers per synthetic batch. However graphite is not a desirable material to use as a growth substrate when developing materials that will contact the body. Therefore more biocompatible particulates such as glass based particles were explored as the particulate growth substrate.

The best particulate substrate for producing biocompatible nanofibers is glass. We explored various glass particulates as a substrate upon which to deposit our growth catalyst and grow nanofibers. We selected a coarse grain glass fiber that was an effective deposition substrate for gold and produced significant quantities of nanofibers in a 2.8" cylindrical growth furnace. Using this approach we were able to load approximately 300grams of growth substrate in the 2.8" furnace tube and increase the mass by approximately 6% indicating that about 18g of silicon and silicon nanofibers are deposited onto the growth substrate during the furnace growth period. Figure 19 shows the reproducibility of this growth rate over 15 separate furnace runs.

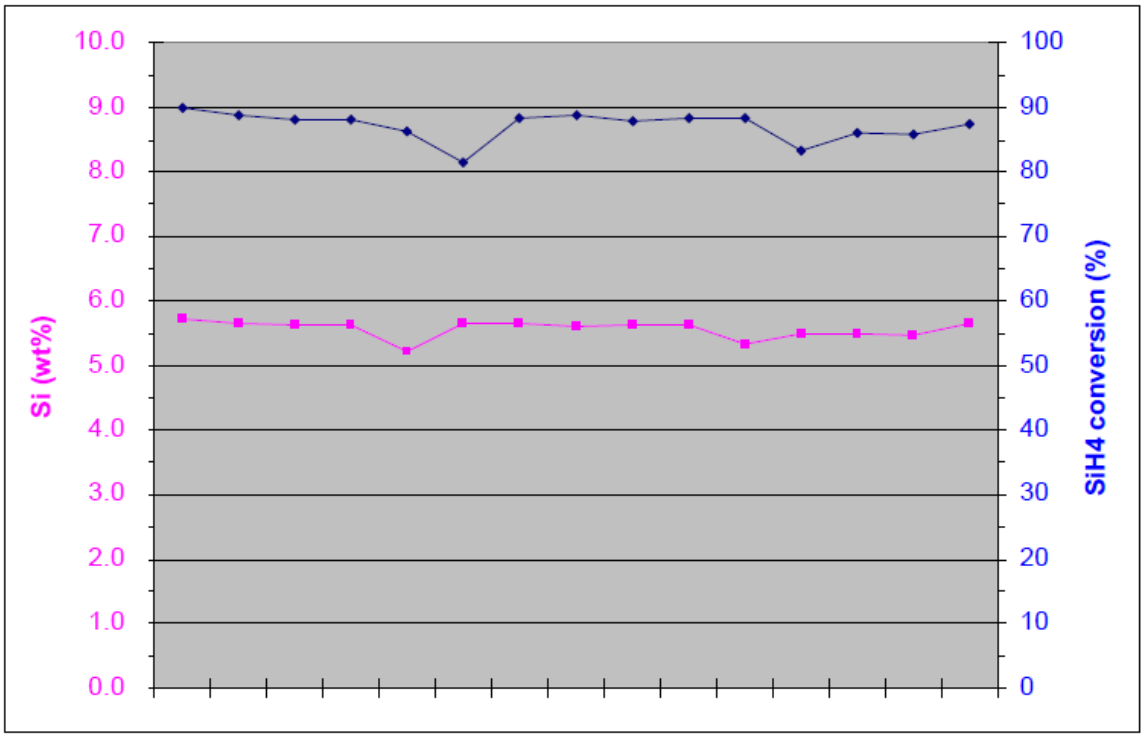

Figure 19 This graph shows the percentage increase in silicon mass of the growth substrate (left axis, lower pink line). At this percentage of nanofibers growth the furnace utilized almost 90% of the injected saline gas, demonstrating the inherent efficiency of the growth parameters used.

The physical appearance of the growth substrate before and after growth can be seen below in figure 20.

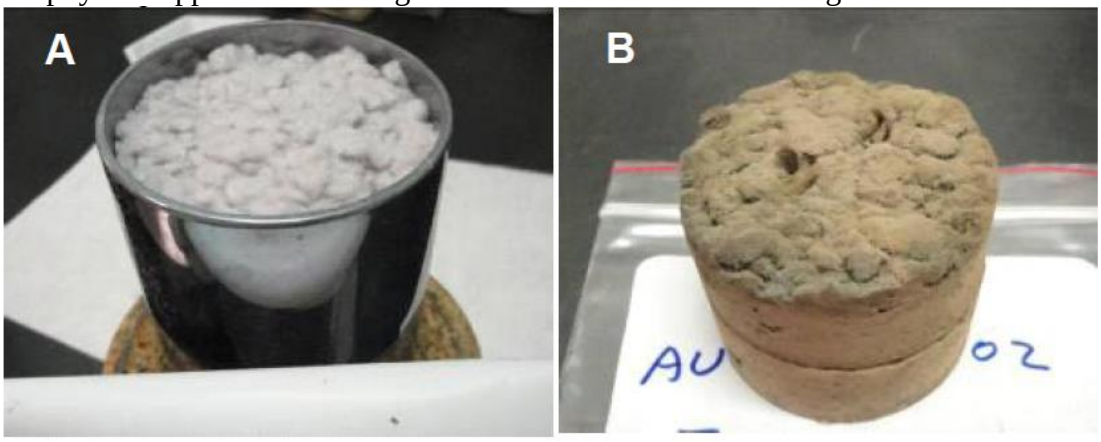

Figure 20 A: shows an image of the growth substrate before loading into the furnace and B: shows the same material after the nanofiber growth (note the change in color of the growth substrate from white to tan).

In order to verify that the material grown on the substrate was predominantly nanofibers we analyzed the substrate in a scanning electron microscope (SEM). Figure 21 shows an SEM image of the growth substrate shown in figure 20B after growth and confirms that there is effective growth of silicon nanofibers onto the growth substrate.

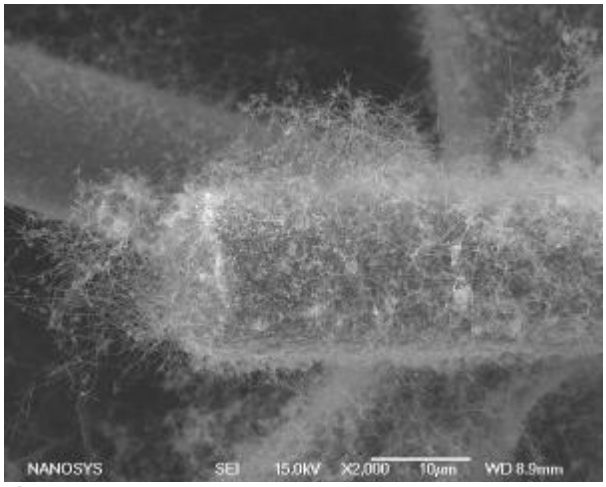

Figure 21. Scanning electron micrograph showing the growth of silicon nanofibers on a large glass particle. Note the dense coating of grown nanofibers on the surface of the substrate. The next section describes how these nanofibers are harvested.

The next step was to evaluate how effectively the nanofibers can be harvested from this growth substrate. Using a combination of sonication and vigorous stirring we were able to harvest approximately 31% of the measured weight increase (Figure 22). This gives an approximate nanofiber yield of 2-3% of the weight of the growth substrate. This means that from a 2.8" growth furnace with 300g of growth substrate we could produce about 6 grams of harvested wires per run.

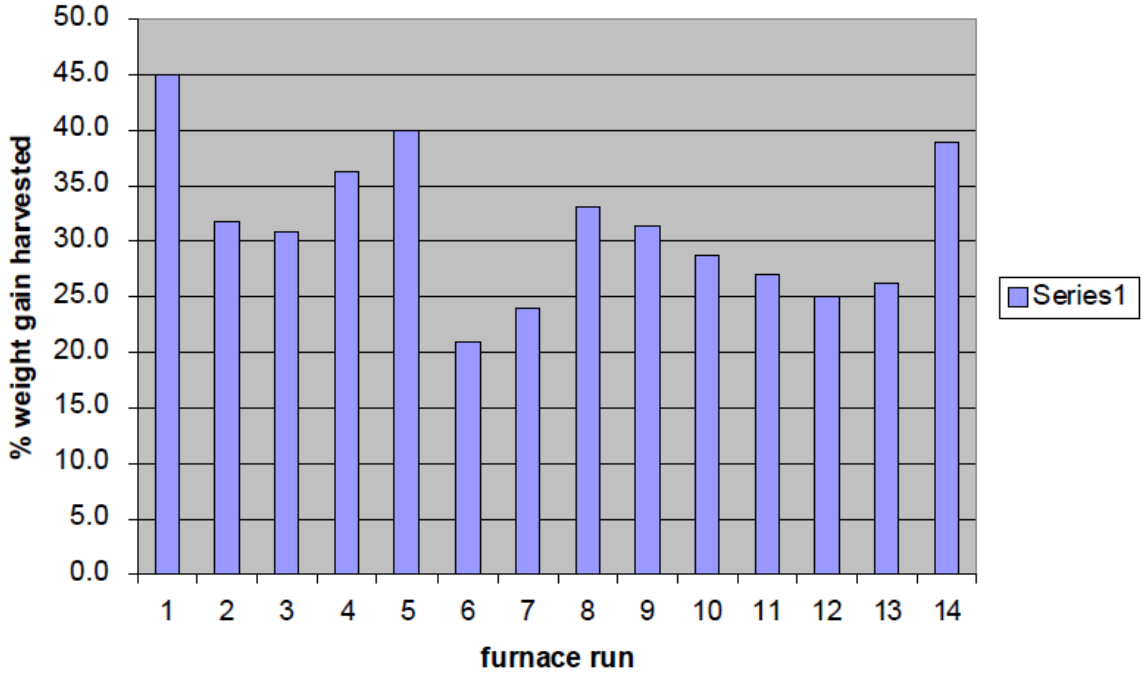

Figure 22 This graph shows the percent of the mass of added Si weight that were harvested as nanofibers from 14 of the 15 furnace runs shown in figure 5. The average silicon mass increase harvested as nanofibers from these 14 runs was 31.4%. This process can likely be optimized further by modifying the nanofibers harvesting process.

At Nanosys we have various sized growth furnaces. Our largest has an 8" tube with an extended growth region. If we were to scale the loading of growth substrate to be equivalent to the 2.8" furnace we can load 3kg of growth substrate into this furnace. Assuming growth and harvesting scale as expected this would yield approximately 60grams of nanofibers from a single furnace run. It would be straight forward to complete 2 furnace runs in a single working shift. Thus with this method of growth we can easily achieve our goal of >100g nanofibers per day. Furthermore, we have demonstrated (using graphite as a growth substrate) that mass

increases of 10% can be achieved by varying gas injection and utilization rates and we have also demonstrated that harvesting rates of up to 45% of this mass can be achieved. If the process were optimized to routinely achieve these numbers then a single run in an 8” furnace could yield >130grams of nanofibers.

Subtask 4b Scale up bandage process to achieve >200g per day

Following the harvesting of the nanofibers into a coating solvent the next step is to apply the nanofibers to a dressing substrate. As described in the sections above the dressing could be made of any material that is compatible to our coating solvent. Examples include gelatin based and cellulose based substrates. The process we have developed involves immersing the dressing substrate into a coating solvent such that it absorbs the solvent carrying the nanofibers onto and into the dressing. After this the solvent is evaporated away leaving a dressing coated with nanofibers. Because of the low mass and high surface area of the nanofibers the intermolecular forces that bring them to the dressing material are readily strong enough to prevent the nanofibers from dislodging. Most of the dressing substrates evaluated to date absorb about 100 microliters of solvent per square centimeter. Thus to get a loading density of 0.5mg/sq.cm (a value we had previously demonstrated achieves good coagulation without affecting material handling) we would typically immerse the dressing substrate in 5mg/ml nanofibers in coating solvent (typically alcohol).

Figure 23 below shows a schematic diagram of our scaled up coating system. As the diagram shows the ideal format for the uncoated dressing is as a roll that can be continuously processed through the coating and drying system. We have not yet obtained a supply of the gelatin or collagen as a roll so we have manually placed the materials in a batchwise process into the coating trough and placed in the drying chamber. The carboxymethylcellulose is available as a roll and thus can be coated in the manner we envisioned.

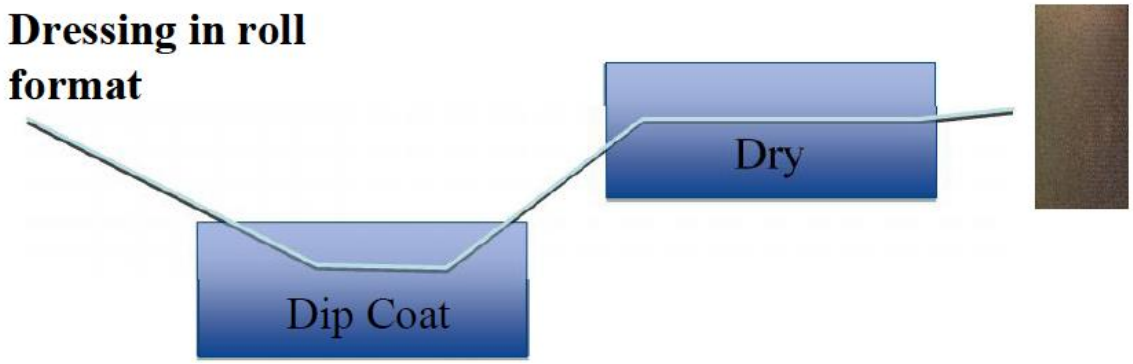

Figure 23: Schematic diagram of the coating process. The blue line represents a continuously moving dressing that is driven through the dip coating solvent and oven by a conveyor. The output is dry, coated dressing.

We have assembled a prototype of this system and that can be seen in figure 24. The prototype involves the use of a standard “pizza oven” with a conveyor that is used to drag the dressing material through the coating solution and oven. This system has been used to successfully produce coated dressings. The throughput of a single system of this size is approximately 100 bandages a day. Therefore, scaling either the size of the oven or using duplicate lines can achieve a scaled up production of coated dressings in line with the task goal.

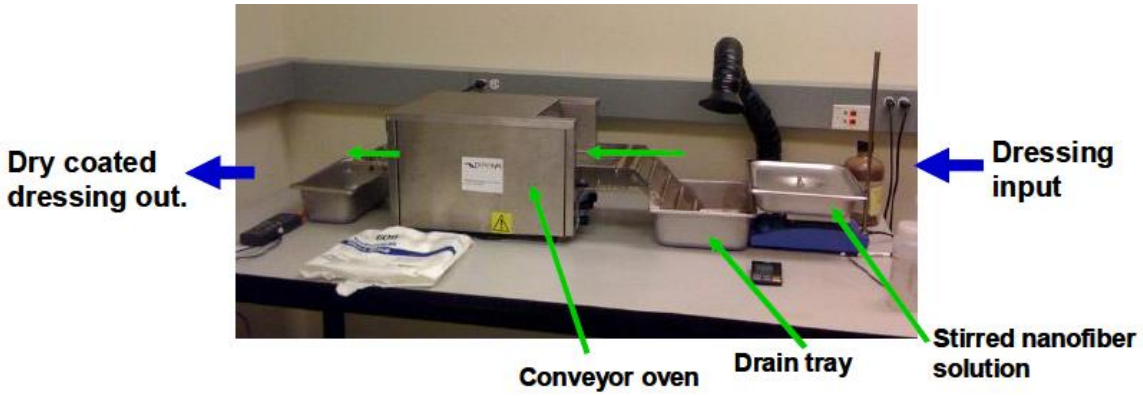

Figure 24: Roll to roll dressing coating prototype. This picture shows the prototype dressing coating system utilizing a conveyor oven to pull the dressing material through a coating solution and into a drying chamber. The output material can be cut to size, folded and packaged as needed.

As described above, throughput that could be attained with a single coating system is approximately 100 bandages per day. Therefore scaling of this process to 200 per day could be simply achieved by adding an additional coating system.
In addition, we have initiated discussions with web converting companies in order to evaluate the potential throughput of this coating approach. These discussions suggest that a method like this could be easily adapted to produce thousands of bandages a day with a larger version of the coating system, in-line cutting and packaging of the bandages.

Y1 Objective 5 Develop relevant severe injury models representative of the types of severe internal trauma that must be treated in combat surgical settings. Fully implement both acute and chronic studies using these models for year 2 demonstrations of hemostatic efficacy, safety and resorption of hemostatic nanofiber dressing Months 9-12.

The primary aim of this goal was to initiate a relationship with relevant thought leaders in the US military to identify appropriate models to test in year 2 of this program. Our current understanding is that there is no identified funding mechanism for year 2 of this program and hence this activity has not been initiated. It can be assumed that we will reach out to the appropriate testing bodies should a funding mechanism be identified.

KEY RESEARCH ACCOMPLISHMENTS

1. We tested three substrates in our standard swine injury model. The gelatin sponge appears to be the promising material as a fully resorbable/biocompatible carrier matrix.
2. We in situ demonstrated that the resorption of the nanofiber dressing
3. We determined that the integrated nanofiber hemostat has no significant toxic effects to cells or tissues using cell based and small animal models
4. We developed effective surface functionalization strategies that allow additional functionality to be attached to the nanofibers.
5. We demonstrated that nanofibers can be manufactured at >100 g/day and demonstrate a process for integrating nanofibers into resorbable dressing materials that can produce >200 bandages/day.

REPORTABLE OUTCOMES

The nano hemostat based on nanofibers has a good resorption and tolerable toxicity and would be useful for future development as a battlefield nano hemostat product.

CONCLUSION

We have developed functional silicon nanofibers that can be effectively integrated into the resorbable dressing materials. The silicon nanofiber samples were less easily resorbed than the gelform only samples. The smallest of the samples was almost completely resorbed by 8 weeks the larger ones were not. This suggests that the nanofibers can be resorbed but we would likely need to limit the amount of material left in for effective resorption. The silicon nanofibers did not cause any major irritation or inflammatory response, and may represent new formats of hemostat materials that can quickly and effectively stop bleeding at the battlefield.

REFERENCES

Conference presentation:

Fei Tian, Xu Wu, Kali Shephard, Aaron Hanson, Min Wu[†], R. Hugh Daniels [‡], Julia Xiaojun Zhao*, Surface Modification of Hemostatic Silicon Nanofiber for Anti-Microbial Functionality, NDEPSCoR Annual Conference, Grand Forks, ND, 09-22,2012

Fei Tian, Xu Wu, Kali Shephard, Aaron Hanson, Min Wu[†], R. Hugh Daniels [‡], Julia Xiaojun Zhao*, Surface modification of hemostatic silicon nanofibers to provide anti-microbial functionality, Pittcon 2013, Philadelphia, March 2013

Invited speaker in symposium of Journal of Nanomedicine Summit, Nanotech Expo 2013, May 12-15. Development of novel nanoparticles for improved imaging, photo-thermotherapy, drug package, and targeting delivery. **Min Wu***, Jiao Chen, Xuefeng Li*, Xu Wu, Nenny Fahruddin, and Julia Xiaojun Zhao.

APPENDICES

Abstract for the Pittcon 2013, Conference Presentation

Surface modification of hemostatic silicon nanofibers to provide anti-microbial functionality

Fei Tian, Xu Wu, Kali Shephard, Aaron Hanson, Min Wu[†], R. Hugh Daniels [‡], Julia Xiaojun Zhao*
Department of Chemistry, [†]Department of Biochemistry and Molecular Biology, University of North Dakota, ND 58202, and [‡]Nanosys Inc, CA)

The use of functional nanomaterials in biology is one of the fastest developing areas in nanoscience and nanobiotechnology. Silicon nanofibers (SiNFs) have been explored to be a novel material for enhancing the hemostasic capability of wound dressings due to their unique advantages such as huge surface-to-volume ratio, high flexibility and good biocompatibility. Using SiNFs as a substrate, we have produced a novel antibacterial silicon nanofiber with strong antibacterial property while retaining its hemostatic activity. Gentamicin was chosen as the model anti-bacterial agent that could be coupled to the nanostructures to create the hybrid nanostructure. The gentamicin was grafted on the nanofiber surface by surface modification. Different modification methods were evaluated to achieve better conjugation. The hybrid nanostructure was evaluated by SEM, FT-IR and EDS. The results showed that silicon nanofibers have high flexibility and good dispersion in aqua solution. The antibacterial property of SiNFs was evaluated with Pseudomonas aeruginosa as a model microorganism and the gentamicin hybrid nanostructure showed good antimicrobial properties. The hybrid nanostructure was then evaluated for its hemostatic activity and shown to provide equivalent hemostasis to unmodified SiNF.

Development of novel nanoparticles for improved imaging, photo-thermotherapy, drug package, and targeting delivery.

Min Wu*, Jiao Chen, Xuefeng Li*, Xu Wu, Nenny Fahruddin, and Julia Xiaojun Zhao.

* Department of Biochemistry and Molecular Biology, University of North Dakota, Grand Forks, ND 58203-9037, USA; Department of Chemistry, University of North Dakota, Grand Forks, ND 58202, USA.

We have developed novel nanoparticles for biomedical research and practical application, particularly, silica based nanoparticles which may be the nanomaterials with the lowest toxicity. We first describe the synthesis, characterization, and application of novel silica nanowires (SiNWs) covered with a gold shell of tunable thickness. These Au-modified SiNWs gained strong surface plasmon resonance absorption in the near infrared (NIR) region and showed excellent *in vitro* biocompatibility and improved photothermal cancer cell killing efficacy at a low laser irradiation density (0.3 W/cm^2). Thus, these Au-modified SiNWs may be a promising candidate as a hyperthermia agent. Next, we report a facile method of synthesizing hollow silica nanoparticles through the sol-gel process of tetraethylorthosilicate and polyvinylpyridine-water droplets as soft templates. The spontaneous sol-gel process on the surface of the droplets allowed the formation of a hollow structure. We characterized the synthesized hollow silica nanoparticles and examined the underlying mechanism for formation of the hollow-like structure. We investigated the feasibility of encapsulating different molecules (*e.g.* $Ru(bpy)_3^{2+}$ and polymyxin) in the silica matrix for potential medical application. Finally**,** we developed a facial bottom-up method for the synthesis of fluorescent graphene quantum dots (GQDs) by one-step pyrolysis of glutamic acid. The GQDs showed relatively strong blue, green and red photoluminescent (PL) under the irradiation of ultra-violet, blue and green light, respectively. Interestingly, the GQDs emit NIR fluorescence in the range of 800-850 nm in an excitation dependent manner. The quantum yield of GQDs in the blue range was 66.7% when they were irradiated at 360 nm. *in vivo* imaging was then used in nude mice and showed their potential in the bioimaging applications because of their great biocompatibility and low cytotoxicity. In addition, the GQDs show the intrinsic peroxidase-like catalytic activity, which is similar to graphene sheet and carbon nanotubes. Coupled with ABTS, the GQDs can be used for the detection of hydrogen peroxide with the limit of detection of 20 μM. In summary, these three types of novel nanoparticles may have strong potential for imaging, thermotherapy, drug packaging, and targeting delivery.

Funding: DoD TATRIC W81XWH-11-2-0163, NIH AI1101973-01 and FAMRI CIA 103007 grants.